Osteonal effects on elastic modulus and fatigue life in equine bone

V.A. Gibson[a], S.M. Stover[b], J.C. Gibeling[c], S.J. Hazelwood[a], R.B. Martin[a,*]

[a]*Orthopaedic Research Laboratory, School of Medicine, UC Davis Medical Center, 4635 Second Avenue, Sacramento, CA 95817, USA*
[b]*J.D. Wheat Veterinary Orthopedic Research Laboratory, School of Veterinary Medicine, University of California at Davis, Davis, CA 95616, USA*
[c]*College of Engineering, Department of Chemical Engineering and Materials Science, University of California at Davis, Davis, CA 95616, USA*

Abstract

We hypothesized that recently formed, incompletely mineralized, and thus, relatively deformable osteons in the equine third metacarpus enhance in vitro load-controlled fatigue life in two ways. Macroscopically, there is a compliance effect, because reduced tissue elastic modulus diminishes the stress required to reach a given strain. Microscopically, there is a cement line effect, in which new osteons and their cement lines more effectively serve as barriers to crack propagation. We studied 18 $4 \times 10 \times 100$ mm beams from the medial, lateral, and dorsal cortices of metacarpal bones from 6 thoroughbred racehorses. Following load-controlled fatigue testing to fracture in 4 point bending, a transverse, 100 μm thick, basic fuchsin-stained cross-section was taken from the load-bearing region. The number and diameter of all intact (and thus recently formed/compliant) secondary osteons in a 3.8×3.8 mm region in the center of the section were determined. The associated area fraction and cement line length of intact osteons were calculated, and the relationships between these variables, elastic modulus (E), and the logarithm of fatigue life ($\log N_F$) were analyzed. As expected, $\log N_F$ was negatively correlated with E, which was in turn negatively correlated with intact osteon area fraction and density. $(\log N_F)/E$ increased in proportion to intact osteon density and nonlinearly with cement line density (mm/mm^2). These results support the hypothesis that remodeling extends load-controlled fatigue life both through the creation of osteonal barriers to microdamage propagation and modulus reduction.

1. Introduction

The third metacarpal bone of thoroughbred racehorses is an excellent example of the ability of the skeleton to adapt to variable physical activity. We have shown that the mid-shaft cortex of this bone exhibits characteristic regional variations in histological structure that correlate with tissue mechanical properties (Table 1). For example, elastic modulus and static strength are usually greatest in the lateral aspect of the cortex and lowest in the dorsal region, with the medial cortex intermediate, but fatigue life measured in load control follows an opposite pattern (Gibson et al., 1995).

Variations in tissue structure between the lateral and dorsal regions may arise from differences in habitual load bearing. Data from in vivo strain gauging experiments (Gross et al., 1992) have revealed that during trotting at medium speed (3.6 m/s) the neutral axis of this bone rotates and translates within the cortex during the gait cycle such that the most dorsal region remains in tension, but a portion of the lateral region is alternately loaded in tension and compression.

We hypothesize that regional differences in the mechanical properties of the equine third metacarpal bone result from variations in the numbers and structure of secondary osteons (SOs) produced by remodeling in response to physiologic loading (Table 1). For example, we have found that osteons in the dorsal region are smaller and more numerous than those in the lateral

Table 1
Summary of regional variations in mechanical and histomorphometric characteristics of cortical bone from the equine third metacarpus as determined in previous experiments conducted in the authors' laboratories

Variable	Lowest	Intermediate	Highest	Reference
Elastic modulus	Dorsal+	Medial*	Lateral#	Gibson et al. (1995)
Monotonic strength	Dorsal+	Medial*	Lateral#	Gibson et al. (1995)
Osteon diameter	Dorsal+	Medial*	Lateral*	Martin et al. (1996a)
Longitudinal collagen	Dorsal+	Medial+	Lateral*	Martin et al. (1996b)
"Hooped" osteons	Dorsal+	Lateral*	Medial*	Martin et al. (1996a)
Past remodeling	Lateral+	Dorsal+	Medial*	Martin et al. (1996c)
Active remodeling	Lateral	Medial	Dorsal	Martin et al. (1996c)
Porosity	Lateral+	Medial+	Dorsal*	Martin et al. (1996c)
Osteon pullout	Lateral+	Medial+*	Dorsal*	Hiller et al. (2003)
Fatigue life	Lateral+	Medial*	Dorsal*	Gibson et al. (1995)

Within a row, different symbols (*, +, #) indicate statistically significant regional differences.

region, and are associated with more transversely oriented collagen fibers as determined by polarized light (Martin et al., 1996b). Also, osteons having a "hooped" architecture, in which longitudinal inner fibers are surrounded by circumferential outer fibers, are associated with the medial and lateral regions and with high elastic modulus rather than long fatigue life (Martin et al., 1996a). Other examples of regional differences in tissue structure that may affect mechanical properties are evident in Table 1.

We have also observed regional differences in the characteristics of the fractured surfaces of test specimens. The dorsal and medial regions exhibit more "pulling out" of osteons during tensile failure than the lateral region, and pullout is associated with low elastic modulus and long fatigue life (Hiller et al., 2003). Thus, in addition to diminished elastic modulus, superior fatigue resistance is associated with more numerous, smaller osteons that "pull out" during fracture.

It has long been proposed that osteons act as toughening fibers in bone, similar to engineered fiber–matrix composite materials (Carter et al., 1976; Currey, 2002; Guo et al., 1998; Hogan, 1992). We are especially interested in the mechanical effects of variability in the elastic properties of the osteonal fibers in relationship to the interstitial bone. Currey (1975) has shown that the elastic modulus of cortical bone is substantially decreased in proportion to the extent of osteonal remodeling. We assume that more recently formed osteons are more compliant than older osteons because the secondary mineralization of new bone tissue continues over an extended period of time following its initial formation and primary mineralization (Boivin and Meunier, 2002; Parfitt, 1983). It is also reasonable to assume that osteons with intact cement lines are, on average, younger and therefore more compliant than osteons that have been partially "overlapped" by more recent remodeling activity (Parfitt, 1983; Rho et al., 2002) (Fig. 1, top; Fig. 2). Thus, we have a conceptual model in which young, intact, relatively compliant
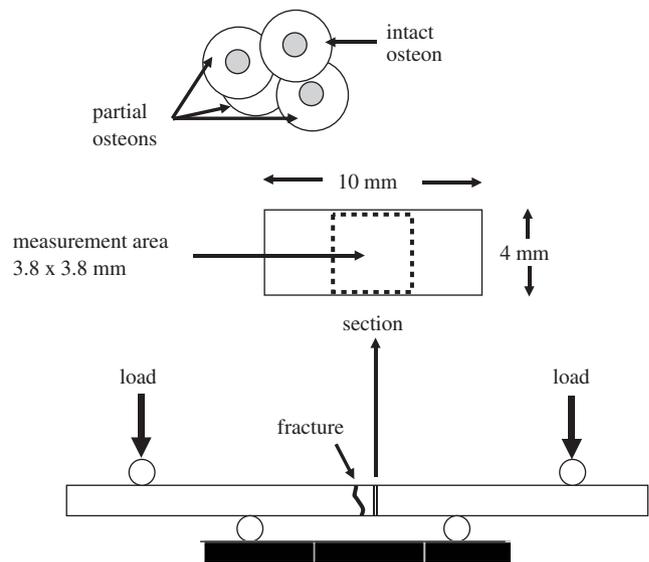

Fig. 1. Geometry of the four-point bending fatigue test and the location of the histomorphometric test section in the beam are shown in the bottom portion of the figure. The middle portion of the figure shows the 3.8 × 3.8 mm analysis region in the 4 × 10 mm test section, and the top sketch illustrates how intact osteons were distinguished from previously formed osteons that have been overlapped by more recent remodeling events.

osteons are embedded in an interstitial matrix of older, more mineralized, and stiffer partial osteons and osteonal remnants.

Using this model we studied the relationships between osteonal numbers and dimensions and two interrelated mechanical properties: elastic modulus and fatigue life. We hypothesized that the effects of osteonal remodeling on these properties involve two specific mechanisms.

● Compliance effect: new osteons, having a low degree of mineralization, are associated with a low elastic modulus of the composite bone tissue. This in turn should lead to a long fatigue life under load control to a given initial strain because the applied peak load is reduced.
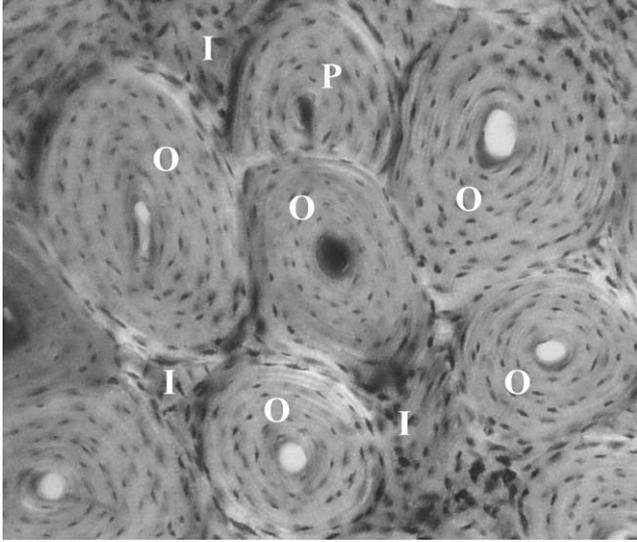
Fig. 2. Typical osteonal structure in the equine third metacarpal specimens studied here. Representative osteons that would have been considered intact in this study are labeled O, one considered a partial osteon is labeled P, and interstitial regions are labeled I.

- Cement line effect: if the compliance effect is accounted for by normalizing $\log N_F$ by elastic modulus, there should remain a significant positive correlation between modulus-normalized fatigue life and the total cement line length of intact osteons because these cement lines represent barriers to the propagation of microcracks to a critical length (Boyce et al., 1998; Martin and Burr, 1989).

2. Methods

Eighteen beams measuring $4 \times 10 \times 100$ mm were machined from the left third metacarpal bones of 6 thoroughbred racehorses. Half the horses were male (one of which was castrated). The horses' age range was 3–5 years, with 4 of the animals being 4 years old. A single beam was cut from each lateral, dorsal, and medial cortex.

The long axes of the beams were parallel to that of the bone, and the 10 mm faces were perpendicular to a radius vector from the center of the diaphysis. Each beam was loaded to fatigue failure under load control in four-point bending using symmetrically arranged roller supports (Fig. 1, bottom). A single load cycle to 200 N was applied at 2 Hz to determine the specimen's initial elastic modulus. Sinusoidal fatigue loading was then conducted in load control at 2 Hz to a peak load calculated to produce an initial peak strain range of 0–10,000 microstrain. Loading occurred in a calcium-buffered saline bath at 37 °C. Other details of the loading methods were previously reported (Gibson et al., 1995). The initial elastic modulus and the number of cycles to failure (defined as fracture) were recorded as E and N_F, respectively.

The failed beam fragments were sequentially soaked for 24 h in 1% basic fuchsin in 70%, 80%, 90% and 100% alcohol (Burr and Stafford, 1990). They were then soaked for an additional 24 h in a 100% alcohol, 1% basic fuchsin solution before being dried in air for a minimum of 48 h and rehydrated in de-ionized water. A transverse section was cut from each beam using a Gillings-Hamco diamond saw. Complete cross-sections were taken as close to the center of the beam as possible without encountering any part of the fracture surfaces. The sections were initially cut to a thickness of ~250 μm, then hand ground to 100 ± 5 μm with 600 grit sand paper and mounted on glass slides using Eukitt (Calibrated Instruments, Inc., Hawthorne, NY). Histomorphometric analysis was conducted within a 3.8×3.8 mm region that spanned nearly the entire central region of the beam cross-section (Fig. 1, middle) using a Model AHBT Vanox-T microscope (Olympus, Tokyo, Japan) with $10 \times$ and $20 \times$ objectives. The area of the analysis region was defined as B.Ar $= 3.8^2 = 14.44$ mm^2.

The specimens were highly remodeled so that few primary osteons remained. Within the analysis region, SOs were identified by their prominent cement lines. Intact SOs were defined as those with an intact cement line (i.e., not overlapped by a later osteonal remodeling event; Fig. 1, top; Fig. 2). As noted above, we were only interested in measuring osteons with intact cement lines because they will generally have been most recently formed and thus be less mineralized than overlapped or partial osteons. The number of intact osteons in each specimen's analysis region (N.On) was counted and divided by B.Ar to obtain osteon density (On.Dn, #/mm^2)

$$\text{On.Dn} = \text{N.On}/\text{B.Ar}. \tag{1}$$

Osteonal diameter was measured for 10 intact SOs randomly selected from throughout the analysis area of each beam. Two diameters, 90° apart, were measured for each osteon, and mean diameter was calculated for each specimen (On.Dm, μm). The mean area occupied by individual intact osteons (μm^2) was estimated as

$$\text{On.Ar} = (\text{On.Dm})^2 \pi/4. \tag{2}$$

The mean area fraction occupied by intact osteons was then estimated as

$$\text{On.Ar}/\text{B.Ar} = \text{On.Ar} \times \text{On.Dn}. \tag{3}$$

We also studied the effects of cement line interfaces on fatigue life and elastic modulus. For this purpose the aggregate cement line length of *intact osteons* per unit area of cross-section (cement line density, I.Cm.Dn, mm/mm^2) was estimated as

$$\text{I.Cm.Dn} = \pi \text{On.Dm} \times \text{On.Dn}. \tag{4}$$

Regional differences in elastic modulus, fatigue life, and the size, aggregate cement line length, and density of intact osteons were assessed using two-way analysis of variance (ANOVA) with horse and region as fixed factors to account for subject variation. Least-squares means adjusted for the horse effect were examined to detect significant pairwise differences between dorsal, medial, and lateral regions. To adjust for the effect of initial modulus when assessing the effect of fatigue life, initial modulus was incorporated in a model as an additional covariate. In addition, simple linear, multiple linear, and quadratic regression analyses were used to assess relationships between the osteonal and mechanical variables. In all cases, $p < 0.05$ was the criterion for statistical significance.

3. Results

Intact osteon density was 62% greater in the dorsal region than in the lateral region, with the medial region not significantly different from either (Table 2). Consistent with this, intact osteons had smaller mean diameters in the dorsal region than in the medial region, with the lateral region intermediate. Because the more numerous osteons in the dorsal region generally had small diameters compared to the other regions, there were no regional differences in mean area fraction or cement line length of intact osteons, although there was a statistical trend for increased cement line density in the dorsal region relative to the lateral region ($p = 0.074$) (Table 3).

There were statistically significant differences in osteonal diameters and area fractions among the experimental horses. Horse least-squares mean osteon diameter, adjusted for region, ranged from 158 to 219 μm, with the former value being significantly smaller than those of all the other horses. Across horses mean osteon area fractions adjusted for region ranged from 20.1% to 56.9%, with horses at the extremes significantly different from each other. However, horse was not statistically significant as a main effect ($p = 0.072$).

Table 2
Experimental data

Horse	Osteon dia. (μm)	Osteon density (#/mm²)	Ost area fraction (%)	Cem line density (mm/mm²)	Initial elastic modulus (Gpa)	Fat. life N_F cycles	Log N_F	Log N_F/E (GPa⁻¹)
Dorsal region								
1	190	23.55	66.8	14.05	16.1	771	2.887	0.179
2	170	15.51	35.2	8.29	17.9	78	1.892	0.106
3	148	5.61	9.7	2.61	21.1	584	2.766	0.131
4	193	16.69	48.8	10.12	18.4	1320	3.121	0.170
5	189	18.28	51.3	10.86	17.8	600	2.778	0.156
6	167	23.20	50.8	12.17	15.5	6407	3.807	0.246
Mean	*176*[A]	*17.14*[B]	*43.8*	*9.68**	*17.8*[C]	*1627*	*2.875*	*0.165*[E]
SD.	*18*	*6.56*	*19.5*	*3.97*	*1.97*	*2376*	*0.619*	*0.048*
Medial region								
1	214	15.03	54.1	10.10	17.5	1964	3.293	0.188
2	204	11.77	38.5	7.55	20.8	408	2.611	0.126
3	172	14.75	34.3	7.97	19.7	967	2.985	0.152
4	240	14.75	66.7	11.12	20.7	573	2.758	0.133
5	206	16.90	56.3	10.94	17.2	4059	3.608	0.210
6	201	11.29	35.8	7.13	20.5	921	2.964	0.145
Mean	*206*[A]	*14.08*	*47.6*	*9.13**	*19.4*	*1482*	*3.037*[D]	*0.159*
SD	*22*	*2.14*	*13.3*	*1.79*	*1.64*	*1374*	*0.363*	*0.033*
Lateral region								
1	221	12.95	49.7	8.99	18.2	436	2.639	0.145
2	208	10.39	35.3	6.79	20.5	364	2.561	0.125
3	155	8.66	16.3	4.22	22.8	183	2.262	0.099
4	—	—	—	—	23.8	321	2.507	0.105
5	221	13.37	51.3	9.28	20.3	342	2.534	0.125
6	170	7.34	16.7	3.92	21.4	215	2.332	0.109
Mean	*195*	*10.54*[B]	*33.8*	*6.64**	*21.2*[C]	*310*	*2.473*[D]	*0.118*[E]
SD	*30*	*2.63*	*17.0*	*2.54*	*1.98*	*95*	*0.145*	*0.017*

The fatigue lives of bone and other materials generally exhibit a Weibull rather than a normal distribution (Hertzberg, 1993). Therefore, it is useful to express fatigue life as the logarithm of the number of cycles to failure, log N_F. Bold means and standard deviations within a column indicate significant regional differences; see *p*-values in footnote.
A: $p = 0.044$; B: $p = 0.025$; C: $p = 0.007$; D: $p = 0.035$; E: $p = 0.036$.
*Lateral different from dorsal ($p = 0.012$) and medial ($p = 0.031$) when elastic modulus is used as a covariate.

Table 3
ANOVA p-values for effects of horse and region on the experimental variables

	Osteon dia. (µm)	Osteon density (#/mm²)	Ost area fraction (%)	Cem line density (mm/mm²)	Initial elastic modulus (Gpa)	Fat. life N_F cycles	Log N_F	Log N_F/E (GPa⁻¹)
Horse	0.001	0.376	0.010	0.072	0.376	0.612	0.415	0.306
Region	0.113	0.088	0.239	0.165	0.005	0.359	0.099	0.067

Follow-up P-values for specific regional differences in initial elastic modulus were: D vs. $L = 0.002$, D vs. $M = 0.069$, L vs $M = 0.048$. Follow-up P-values for specific differences in osteon diameter and area fraction among the horses are not reported because the specific horses were unique to this experiment.

Elastic modulus and fatigue life were regionally dependent in ways that were consistent with previously studied equine specimens (Gibson et al., 1995). The elastic modulus of the lateral region was significantly greater than that of the dorsal region, with the medial region having intermediate values (Table 2). Lateral specimens had significantly shorter fatigue lives (expressed as log N_F to obtain a normal distribution of the data) than medial specimens, with dorsal specimens having intermediate fatigue lives. (This was different from our previous results (Gibson et al., 1995), in which the dorsal specimens had the longest fatigue lives, but in both experiments the lateral specimens had the shortest fatigue lives.) When this ANOVA was repeated with elastic modulus as a covariate the significance level was slightly improved ($p = 0.025$), and log N_F had a linear, negative relationship with initial elastic modulus (Fig. 3, $R^2 = 0.335$, $p < 0.012$). In addition, $(\log N_F)/E$ was significantly greater in the dorsal region than in the lateral region ($p = 0.036$), and the medial region was nearly so ($p = 0.062$).

Initial elastic modulus was strongly related to intact On.Dn (Fig. 4); across cortical regions, intact osteon density accounted for three-quarters of the variability in modulus. Modulus was linearly related to intact osteonal area fraction (Fig. 5), but not nearly as strongly as to osteon density. Linear regression analysis did not show a significant relationship between modulus and osteonal size, alone or together with osteonal density.

Log N_F was positively, but weakly, linearly related to intact osteon density ($R^2 = 0.285$, $p = 0.027$), but not to osteonal area fraction, alone or together with osteon density. When log N_F was normalized by elastic modulus to account for the effects of stiffness variation on fatigue life, $(\log N_F)/E$ was not significantly related to mean osteonal diameter, alone or together with osteonal density. On the other hand, $(\log N_F)/E$ was linearly related to intact osteon area fraction ($R^2 = 0.323$, $p = 0.017$) and substantially more strongly related to intact osteon density (Fig. 6). Thus, across cortical regions, intact osteon density accounted for more than half of the variability in log N_F adjusted for elastic modulus variability.
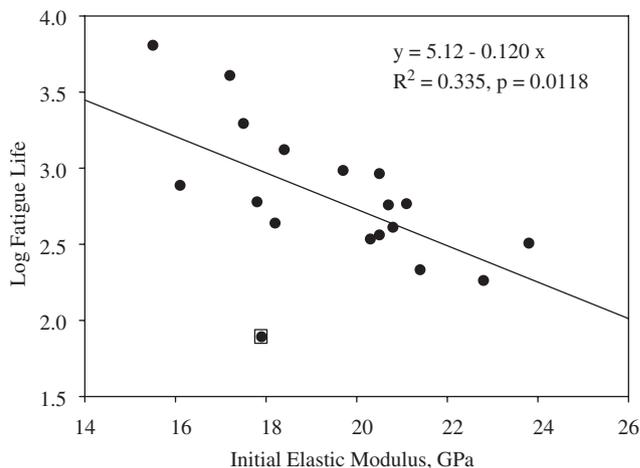

Fig. 3. Linear regression of log N_F vs. initial elastic modulus. Regression data shown in graph are for all data points. If the outlying dorsal region specimen shown in a box is removed from the analysis, $R^2 = 0.590$, $p = 0.0003$, and the regression equation is $y = 5.60 - 0.141x$.

y = 5.12 - 0.120 x
$R^2 = 0.335$, p = 0.0118
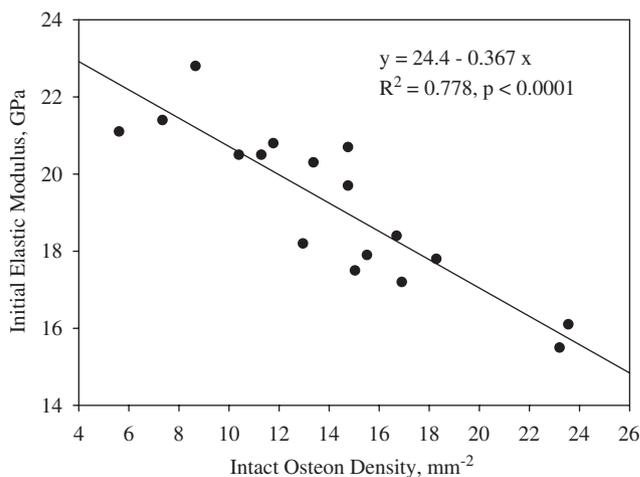

y = 24.4 - 0.367 x
$R^2 = 0.778$, p < 0.0001

Fig. 4. Linear regression results and graph of initial elastic modulus vs. intact osteon density for the 17 specimens with histomorphometric data.

Finally, we examined the relationship between $(\log N_F)/E$ and the calculated total cement line density of intact osteons, I.Cm.Dn (Fig. 7). The linear relationship between these variables was quite significant
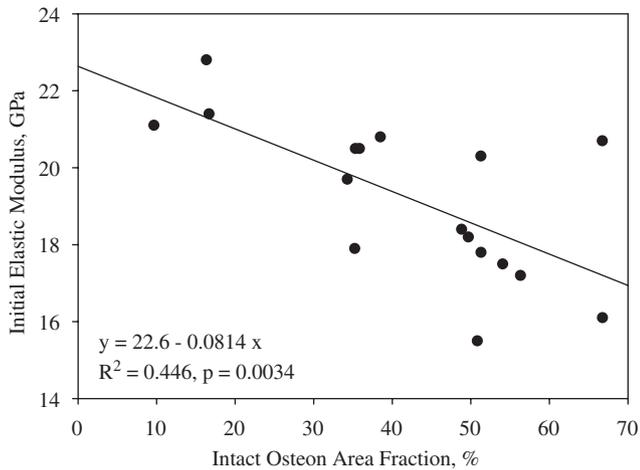
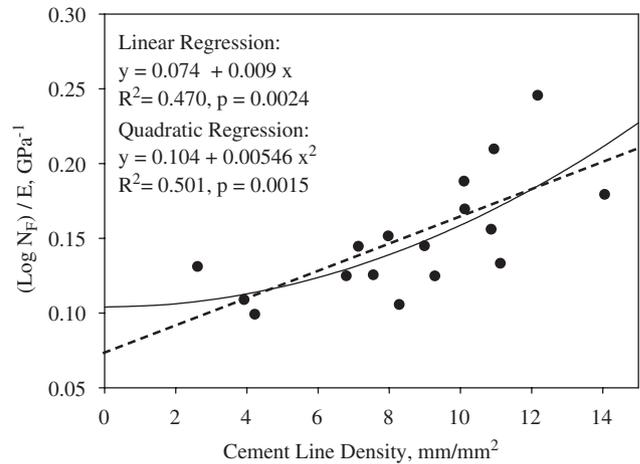Fig. 5. Linear regression of elastic modulus vs. intact osteon area fraction.

y = 22.6 - 0.0814 x
$R^2 = 0.446$, p = 0.0034

Fig. 7. Log N_F normalized by elastic modulus vs. intact cement line density (i.e., calculated total length of intact osteonal cement lines per mm^2 of cross-section). Linear and quadratic regression line data are shown.

Linear Regression:
y = 0.074 + 0.009 x
$R^2 = 0.470$, p = 0.0024
Quadratic Regression:
y = 0.104 + 0.00546 x^2
$R^2 = 0.501$, p = 0.0015
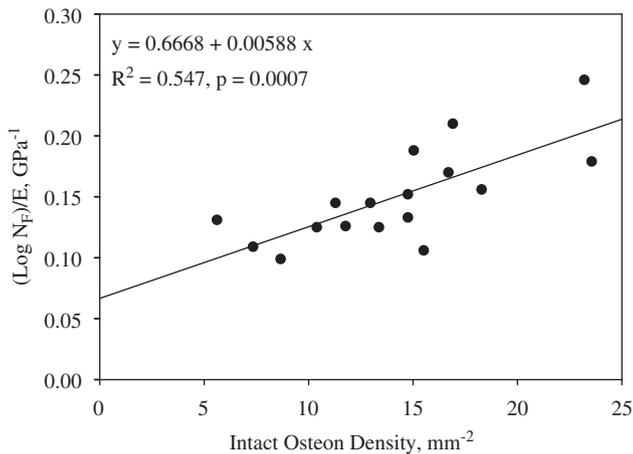

y = 0.6668 + 0.00588 x
$R^2 = 0.547$, p = 0.0007

Fig. 6. When log N_F is normalized by elastic modulus, the result is linearly correlated with intact osteon density. This suggests that osteons affect fatigue life in ways other than through alteration of the specimen's elastic modulus.

($R^2 = 0.470$, $p = 0.002$), but the data were distributed in a somewhat curvilinear fashion. A slightly better correlation was obtained using the quadratic regression relationship shown in Fig. 7 ($R^2 = 0.501$, $p = 0.002$). Although the cortical region by itself was not a significant determinant of intact osteon cement line density, when regional variation in elastic modulus was accounted for by using modulus as a covariate in an ANOVA, I.Cm.Dn was significantly greater in the dorsal ($p = 0.012$) and medial ($p = 0.031$) regions than in the lateral region.

4. Discussion

We hypothesized that the effects of osteonal structure on the elastic modulus and load-controlled fatigue resistance of cortical bone include a compliance effect, in which larger numbers of recently formed, compliant osteons reduce the applied load for fatigue at a given initial strain, thereby increasing the fatigue life, and a cement line effect, in which osteons serve as barriers to crack propagation. The experimental results confirmed that load-controlled fatigue life is significantly increased in more compliant specimens, and that elastic modulus was strongly and negatively correlated with intact osteon density. These outcomes were predictable at the outset. However, the outcomes shown in Figs. 6 and 7 were not: when the compliance effect was accounted for by normalizing log N_F by initial elastic modulus, strong positive effects remained for both the numbers of osteons and their calculated cement line length per unit cross-sectional area. This supports the hypothesis that intact osteons increase load-controlled fatigue life by means other than reducing elastic modulus.

This study has several important limitations, beginning with the relatively small sample size: 18 specimens from 6 horses. However, on average over 200 osteons were studied in each individual specimen, providing a good sample of their numbers and sizes, and the present results are consistent with results from other studies of entirely independent specimens (Table 1). A second limitation involved the experimental loading of the specimens. In vivo strain measurements demonstrate that stresses vary within the equine third metacarpal bone as the horse runs (Gross et al., 1992), and the nature and distribution of the stresses imposed in our fatigue tests were certainly different from those that the specimens had experienced, and presumably adapted to, in the living bone. However, it was not practical to attempt to reproduce the physiologic loading in the specimens.

Another limitation arises from the fact that our fatigue testing was done in load control. We preferred this to deflection (or strain) control for two reasons. First, deflection controlled testing typically results in poorly defined failures because specimens often yield until their plastic deflection equals the defined deflection limit without explicitly fracturing (Gibson, 2000). The second is a physiologic argument: fatigue fractures typically result from circumstances in which the bone is loaded in proportion to body weight, which is more-or-less constant.

When load control is used to fatigue specimens of defined geometry, one can load them all to the same load (or stress) level, or adjust the load to each specimen's stiffness so that they all experience the same strain *at the start of the test*. We assumed that the latter method is more physiologic in the light of experiments showing that peak physiologic strains across vertebrate species are relatively constant (Rubin and Lanyon, 1984).

While we appealed to physiologic principles in defining our fatigue protocol, it was impractical to actually test using physiologic strains (and strain rates) because each test would last an impractically long time (weeks). Therefore, based on previous work (Gibson, 2000), we chose 10,000 microstrain as the initial peak strain because it was high enough to produce fatigue failure in a reasonable period of time (<1 week), but consistently below the yield strain for all 3 anatomic regions.

The fact that $(\log N_{F})/E$ correlated more strongly with the density (Fig. 6) than the area fraction of intact osteons, and did not significantly correlate with measures of osteon size, suggests that the effects of osteons on fatigue life involve factors related to their existence as entities or objects in the material as well as their volumetric contribution to mechanical properties. Fig. 7 suggests that osteonal cement lines strongly influence modulus-normalized fatigue life, but clearly intact osteon density and the density of their cement lines are not independent variables. Nevertheless, these results are consistent with proposed mechanisms for osteonal control of fatigue damage, as follows.

Several authors have hypothesized that the cement lines of adjacent intact osteons help to confine crack propagation within zones of interstitial bone (Burr et al., 1988; Martin and Burr, 1989; O'Brien et al., 2003). In concert with this, Guo et al. (1998) showed analytically that interstitial microcracks should be attracted to osteons that are less stiff than the matrix, and repelled from those that are more stiff. They interpreted this to imply that cracks are induced to propagate toward the cement lines of less mineralized, more compliant osteons, and be arrested there. Conversely, cracks would more readily propagate to a critical length in bone having fewer "young," less mineralized (i.e., intact) osteons. Thus, numerous, recently formed osteons bordering relatively small, more highly mineralized and thus crack-prone interstitial zones (such as those in Fig. 2) should extend fatigue life by allowing strain energy to be dissipated in forming interstitial cracks that are unlikely to grow to a critical length. This is consistent with the observation that about 80% of microcracks in cortical bone lie in interstitial regions (Norman and Wang, 1997; Schaffler et al., 1995) where they are hypothesized to increase fatigue life by reducing strain energy and relieving stress concentrations (Akkus et al., 2000; Vashishth et al., 1997). It is also consistent with the positive association seen here between longer modulus-adjusted fatigue lives and increased numbers of intact osteons (Fig. 6).

In addition to controlling microcrack propagation early in the fatigue failure process, intact osteons' cement lines and their shear properties may be important in increasing the amount of energy required to fracture a bone. Hiller et al. (2003) observed that the fatigue life of equine third metacarpal bone is proportional to the amount of osteonal pullout on the fracture surface. Also, the dorsal region exhibited more osteonal pullout than the medial and lateral regions. Osteonal pullout on fracture surfaces implies shear failure at or near osteonal cement lines, and has been theoretically associated with smaller osteons (Moyle and Bowden, 1984). In the present study, the dorsal region exhibited longer fatigue lives and smaller and more numerous osteons than the other cortical regions, consistent with our previous results (Martin et al., 1996c).

The relationships between osteons' diameters, their tendency to pull out during fracture, and the energy needed to produce fracture, were originally considered analytically by Pope and Murphy (1974), who concluded that osteons of *larger* diameter were more likely to pull out than those of smaller diameter because their tensile strength was greater in proportion to their cement line shear strength. However, Moyle et al. (1978) subsequently performed an experiment showing that the opposite was true: stable, energy-consuming crack propagation during monotonic fracture occurred in regions containing smaller osteons. The latter result is consistent with our own observation associating increased osteonal pullout during fatigue failure with smaller osteons (Hiller et al., 2003). Other work (Moyle and Bowden, 1984) supports the concept that energy dissipation during fracture depends on *both* the likelihood of pullout (which increases for larger osteons) and the number of osteons present (which increases for smaller osteons). Some studies have obtained mixed results. In human cortical bone, Yeni et al. (1997) found that both tensile and shear fracture toughness were inversely proportional to osteon size, and increased in proportion to osteonal density in the femur, but not the tibia.

Fig. 7 suggests that modulus-adjusted fatigue life increases with intact osteons' cement line density, the product of their numerical density (osteons/mm^2) and their mean circumference. While larger osteons have longer cement lines, fewer of them can be packed into a given cross-section. If circular osteons of diameter d in a cross-section $D \times D$ units square were arranged as a square packing array, it would contain $(D/d)^2$ osteons. Because the cement line of each osteon would have length πd, the cement line density in the section would be $\pi d (D/d)^2 = \pi D^2/d$, and the aggregate cement line length would be inversely proportional to osteonal diameter. A similar effect is expected for other packing arrangements or when randomly placed osteons are allowed to overlap one another but only intact osteons' cement lines are considered. While such models are not rigorously consistent with the formation of osteons in bone, they fit the observed trends: intact cement line density was greatest in the dorsal region $(9.68 \pm 3.97\,\text{mm/mm}^2)$, which had osteons of the smallest mean diameter $(176 \pm 18\,\mu\text{m})$, and least in the lateral region $(6.64 \pm 2.54\,\text{mm/mm}^2)$, which tended to have larger osteons $(195 \pm 30\,\mu\text{m})$.

Clearly, biological factors should also govern the range of osteonal dimensions. For example, osteons of large diameter could experience nutrient transport problems from the Haversian canal to their outermost osteocytes, and very small osteons could not have proportionately small Haversian canals because blood vessels must have a minimum functional diameter.

In summary, the data presented here support the concept that osteonal remodeling contributes to the fatigue life of cortical bone not only by removing fatigue damage over time, but also by controlling elastic modulus and creating osteons that promote toughness and interfere with crack propagation. When the effect of remodeling on elastic modulus is discounted by studying modulus-normalized $\log N_{\text{F}}$, it is seen that fatigue life increases with the density of intact osteons and their cement lines, and these variables exhibit characteristic regional variations in the equine third metacarpal bone.

References

Akkus, O., Jepsen, K.J., Rimnac, C.M., 2000. Microstructural aspects of the fracture process in human cortical bone. Journal of Materials Science 35, 1–10.

Boivin, G., Meunier, P.J., 2002. The degree of mineralization of bone tissue measured by computerized quantitative contact microradiography. Calcified Tissue International 70, 503–511.

Boyce, T.M., Fyhrie, D.P., Glotkowski, M.C., Radin, E.L., Schaffler, M.B., 1998. Damage type and strain mode associations in human compact bone bending fatigue. Journal of Orthopaedic Research 16, 322–329.

Burr, D.B., Stafford, T., 1990. Validity of the bulk-staining technique to separate artifactual from in vivo bone microdamage. Clinical Orthopaedics and Related Research 260, 305–308.

Burr, D.B., Schaffler, M.B., Fredrickson, R.G., 1988. Composition of the cement line and its possible mechanical role as a local interface in human compact bone. Journal of Biomechanics 21, 939–945.

Carter, D.R., Hayes, W.C., Schurman, D.J., 1976. Fatigue life of compact bone—II. Effects of microstructure and density. Journal of Biomechanics 9, 211–218.

Currey, J.D., 1975. The effects of strain rate, reconstruction and mineral content on some mechanical properties of bovine bone. Journal of Biomechanics 8, 81–86.

Currey, J.D., 2002. Bones. Structure and Mechanics. Princeton University Press, Princeton, NJ.

Gibson, V.A., 2000. Fatigue behavior of equine third metacarpal bone tissue. Dissertation. University of California, Davis, CA.

Gibson, V.A., Stover, S.M., Martin, R.B., Gibeling, J.C., Gustafson, M.B., Griffin, L.V., 1995. Fatigue behavior of the equine third metacarpus: mechanical property analysis. Journal of Orthopaedic Research 13, 861–868.

Gross, T.S., McLeod, K.J., Rubin, C.T., 1992. Characterizing bone strain distributions in vivo using three triple rosette strain gages. Journal of Biomechanics 25, 1081–1087.

Guo, X.E., Liang, L.C., Goldstein, S.A., 1998. Micromechanics of osteonal cortical bone fracture. Journal of Biomechanical Engineering 120, 112–117.

Hertzberg, R.W., 1996. Deformation and fracture mechanics of engineering materials. Wiley, New York.

Hiller, L.P., Stover, S.M., Gibson, V.A., Gibeling, J.C., Prater, C.S., Hazelwood, S.J., Yeh, O.C., Martin, R.B., 2003. Osteon pullout in the equine third metacarpal bone: effects of ex vivo fatigue. Journal of Orthopaedic Research 21, 481–488.

Hogan, H.A., 1992. Micromechanics modeling of Haversian cortical bone properties. Journal of Biomechanics 25, 549–556.

Martin, R.B., Burr, D.B., 1989. The Structure, Function, and Adaptation of Compact Bone. Raven Press, New York.

Martin, R.B., Gibson, V.A., Stover, S.M., Gibeling, J.C., Griffin, L.V., 1996a. Osteonal structure in the equine third metacarpus. Bone 19, 165–171.

Martin, R.B., Mathews, P.V., Lau, S.T., Gibson, V.A., Stover, S.M., 1996b. Collagen fiber organization is related to mechanical properties and remodeling in equine bone. A comparison of two methods. Journal of Biomechanics 29, 1515–1521.

Martin, R.B., Stover, S.M., Gibson, V.A., Gibeling, J.C., Griffin, L.V., 1996c. In vitro fatigue behavior of the equine third metacarpus: remodeling and microcrack damage analysis. Journal of Orthopaedic Research 14, 794–801.

Moyle, O.D., Bowden, R.W., 1984. Fracture of human femoral bone. Journal of Biomechanics 17, 203–213.

Moyle, D.D., Welborn, J.W., Cooke, F.W., 1978. Work to fracture of canine femoral bone. Journal of Biomechanics 11, 435–440.

Norman, T.L., Wang, Z., 1997. Microdamage of human cortical bone: incidence and morphology in long bones. Bone 20, 375–379.

O'Brien, F.J., Taylor, D., Lee, T.C., 2003. Microcrack accumulation at different intervals during fatigue testing of compact bone. Journal of Biomechanics 36, 973–980.

Parfitt, A.M., 1983. The physiologic and clinical significance of bone histomorphometric data. In: Recker, R.R. (Ed.), Bone Histomorphometry: Techniques and Interpretation. CRC Press, Inc., Boca Raton, FL, pp. 143–223.

Pope, M.H., Murphy, M.C., 1974. Fracture energy of bone in a shear mode. Medical and Biological Engineering 12.

Rho, J.Y., Zioupos, P., Currey, J.D., Pharr, G.M., 2002. Microstructural elasticity and regional heterogeneity in human femoral bone of various ages examined by nano-indentation. Journal of Biomechanics 35, 189–198.

Rubin, C.T., Lanyon, L.E., 1984. Dynamic strain similarity in vertebrates; an alternative to allometric limb bone scaling. Journal of Theoretical Biology 107, 321–327.

Schaffler, M.B., Choi, K., Milgrom, C., 1995. Aging and matrix microdamage accumulation in human compact bone. Bone 17, 521–525.

Vashishth, D., Behiri, J.C., Bonfield, W., 1997. Crack growth resistance in cortical bone: concept of microcrack toughening. Journal of Biomechanics 30, 763–769.

Yeni, Y.N., Brown, C.U., Wang, Z., Norman, T.L., 1997. The influence of bone morphology on fracture toughness of the human femur and tibia. Bone 21, 453–459.